Correlation between superconducting transition temperatures and carrier densities in Te- and S-substituted FeSe thin films

Fuyuki Nabeshima,* Tomoya Ishikawa, Naoki Shikama, and Atsutaka Maeda
Department of Basic Science, The University of Tokyo, Meguro, Tokyo 153-8902, Japan

(Received 11 June 2019; revised manuscript received 30 April 2020; accepted 30 April 2020; published 20 May 2020)

We comparatively investigated the transport properties for S- and Te-substituted FeSe thin films under magnetic fields to clarify the origin of the contrasting behavior of the superconducting transition temperature in S and Te substitution. A classical two-carrier analysis revealed that the carrier densities of the films increased with increasing Te content, while no significant change was observed for the S substitution, which suggests a correlation between T_c and the carrier densities. These observations suggest that the structural transition affects the electronic structure in a different manner between Fe(Se,S) and Fe(Se,Te) and that this fact is the direct cause of the difference in the T_c behaviors at the end point of the structural transition.

DOI: 10.1103/PhysRevB.101.184517

I. INTRODUCTION

Since the discovery of the iron-based superconductors [1], much research has been devoted to reveal the mechanism of superconductivity in these materials. An iron chalcogenide superconductor, FeSe [2] is an iron-based superconductor with the simplest crystal structure, whose superconducting transition temperature, T_c, is 9 K at ambient pressure. It shows a structural transition from tetragonal to orthorhombic phase at 90 K [3], below which an orbital ordered state was observed [4,5]. FeSe exhibits no long-range magnetic order at ambient pressure, while many other iron-based superconductors show a magnetic transition at a temperature very close to the structural transition temperature. Because the structural transition has a possible electronic origin, it is often called the nematic transition and the interplay between nematicity and superconductivity has received much attention [6,7].

A lot of research has been focused on FeSe and S-substituted FeSe because bulk single-crystalline samples are available. With increasing S content, the structural transition temperature decreases, and T_c once slightly increases and then decreases [8–11]. Although no significant change in T_c is observed at the end point of the structural transition, measurements of thermal properties [12] and scanning tunneling microscopy/spectroscopy [13] have revealed an abrupt change in the superconducting gap structure at the end point of the orthorhombic phase, which may suggest the nematic order and its fluctuations have some impact on the superconducting pairing mechanisms.

Rather different behaviors were observed for another isovalent Te substitution for Se. Although bulk samples of $FeSe_{1-y}Te_y$ with $0.1 \leqslant y \leqslant 0.4$ are not available because of phase separation [14], we have demonstrated that the single-crystalline thin films of Fe(Se,Te) in the whole composition region were grown using pulsed laser deposition [15,16]. The structural transition temperature is also decreased by Te substitution, and T_c is largely enhanced at the end point of the structural transition. This behavior of T_c is in contrast to that of $FeSe_{1-x}S_x$, where no such significant change in T_c is observed at the end point of the orthorhombic phase. The contrasting behavior of T_c between S and Te substitution suggests that the nematicity has no universal significance on T_c in these materials [17]. Thus, it is very intriguing to elucidate the origin of the difference in the T_c behaviors between S and Te substitution.

In this paper we report a systematic measurement of Hall effect and magnetoresistance of S- and Te-substituted FeSe thin films. A classical two-carrier analysis revealed a correlation between carrier densities and T_c. Our observation suggests that the structural transition affects the electronic structure in a different manner between Fe(Se,S) and Fe(Se,Te). It also suggests that this fact would be the direct cause of the difference in the T_c behaviors at the end point of the structural transition.

II. METHODOLOGY

All the films were grown on $LaAlO_3$ (LAO) substrates by a pulsed laser deposition method using a KrF laser. Details of the film growth were described elsewhere [17–19]. The thicknesses of the grown films were measured by a Dektak 6 M stylus profiler and by x-ray reflectivity measurement. The electrical resistivity and the Hall resistivity were measured with a standard four-probe method using a physical property measurement system from 2 to 300 K under magnetic fields up to 9 T.

III. RESULTS AND DISCUSSION

Figure 1 shows the temperature dependence of the electrical resistivity of the films. All the films showed the

*cnabeshima@g.ecc.u-tokyo.ac.jp

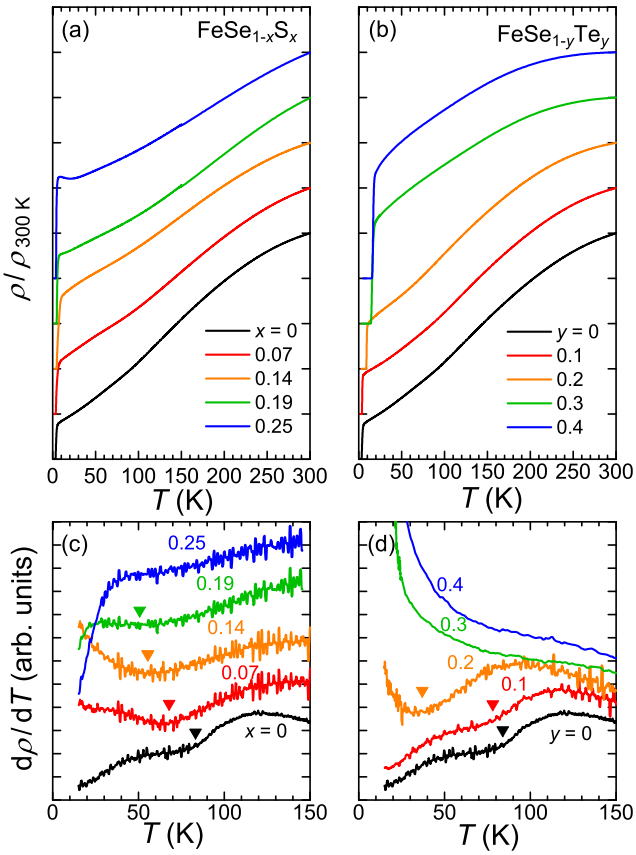

FIG. 1. Temperature dependence of the dc electrical resistivity of (a) the $FeSe_{1-x}S_x$ films on LAO and (b) $FeSe_{1-y}Te_y$ films on LAO. Temperature derivatives of the resistivity of (c) the $FeSe_{1-x}S_x$ films and (d) $FeSe_{1-y}Te_y$ films. Arrows show the anomalies due to structural transition.

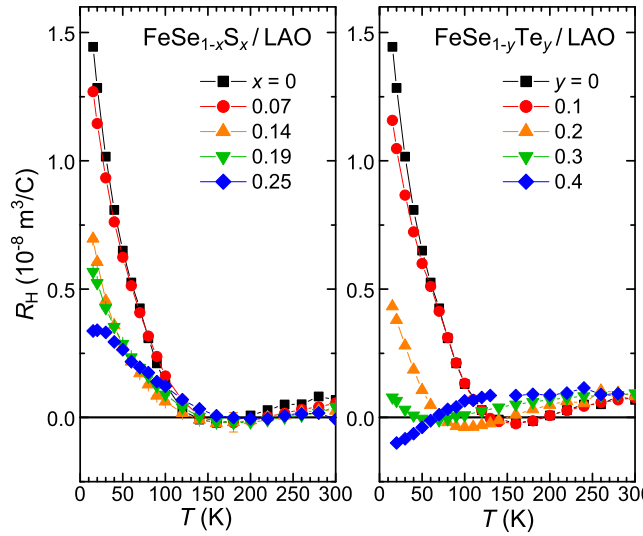

FIG. 2. Temperature dependence of the Hall coefficients, R_H, of the $FeSe_{1-x}S_x$ films (left) and $FeSe_{1-y}Te_y$ films (right).

superconducting transition at low temperatures. T_c of the films are plotted as a function of composition in Fig. 4. Some of the films show different T_c values from bulk values. The differences in T_c are due to the in-plane lattice strain in film samples. FeSe films, for example, show higher T_c under compressive strain and lower T_c under tensile strain than the bulk sample [20]. The tensile strain is the origin of low $T_c^{zero} \sim 3$ K in the FeSe film on LAO in this study. The structural transition temperatures, T_s, of the films were determined by the temperature where anomalous behaviors were observed in the temperature derivative of the resistivity [see Figs. 1(c) and 1(d)]. T_s values decrease with increasing the substitution amount for both S and Te substitution. We observed no signature of the structural transition for films with $x \geqslant 0.25$ or $y \geqslant 0.3$. Although there may be some errors in T_s estimated from the dR/dT curves, we can safely say that the structural transition is present or absent in our samples measured, and our conclusions are not affected. $FeSe_{1-y}Te_y$ films in the tetragonal phase show very high T_c, while $FeSe_{1-x}S_x$ has small T_c values even in the tetragonal phase. Note that a slight upturn behavior was observed at low temperatures in the R-vs-T curve of the $x = 0.25$ film. We observed an upturn behavior with a clear kink in the R-vs-T curve in other films with similar compositions [17], which could be attributed to a magnetic transition because the R-vs-T behavior is very similar to what is observed at the antiferromagnetic transition in FeSe under hydrostatic pressure [21]. Although the upturn in the R-vs-T curve observed in this study is weaker, this would have the same origin.

In our previous paper, we reported that $FeSe_{1-y}Te_y$ films showed T_s of approximately 45 K for $y = 0.3$, while the film with $y = 0.3$ in this study showed no structural transition. This could be attributed to the difference in the strength of the lattice strain between films in the present and previous studies; the film in this study has shorter a-axis length ($a \sim 3.76$ Å) than films in the previous study ($a = 3.77$–3.78 Å) [16]. This is consistent with the fact that the structural transition temperature T_s of FeSe decreases when the strain become more compressive [20]. We also note that we observed the structural transition in $x = 0.19$ film in this study, while we previously observed the structural transition disappeared at $x = 0.18$. This difference could also be attributed to the difference in the strength of the strain. For another possibility, we consider that this may be due to possible deviations in the composition of the grown films. We estimated the composition of the grown films from the nominal composition by using the empirical relation between the nominal and the really measured composition of the films, as described in our previous paper [17]. We consider that the $x = 0.19$ film in the paper has slightly lower S content in reality, just near the boundary between the orthogonal and tetragonal phases.

Figure 2 shows the temperature dependence of the Hall coefficients, R_H, of the $FeSe_{1-x}S_x$ and $FeSe_{1-y}Te_y$ films. R_H of the FeSe film largely increased below $T < 100$ K. The enhancement of R_H at low temperatures was decreased by both S and Te substitution. For Te substitution, R_H at low temperatures becomes very small after the structural transition disappeared. This behavior is very similar to those of $FeSe_{1-y}Te_y$ films on CaF_2 substrates [22]. On the other hand, no significant change in R_H was observed between the films with and without the structural transition in the case of S

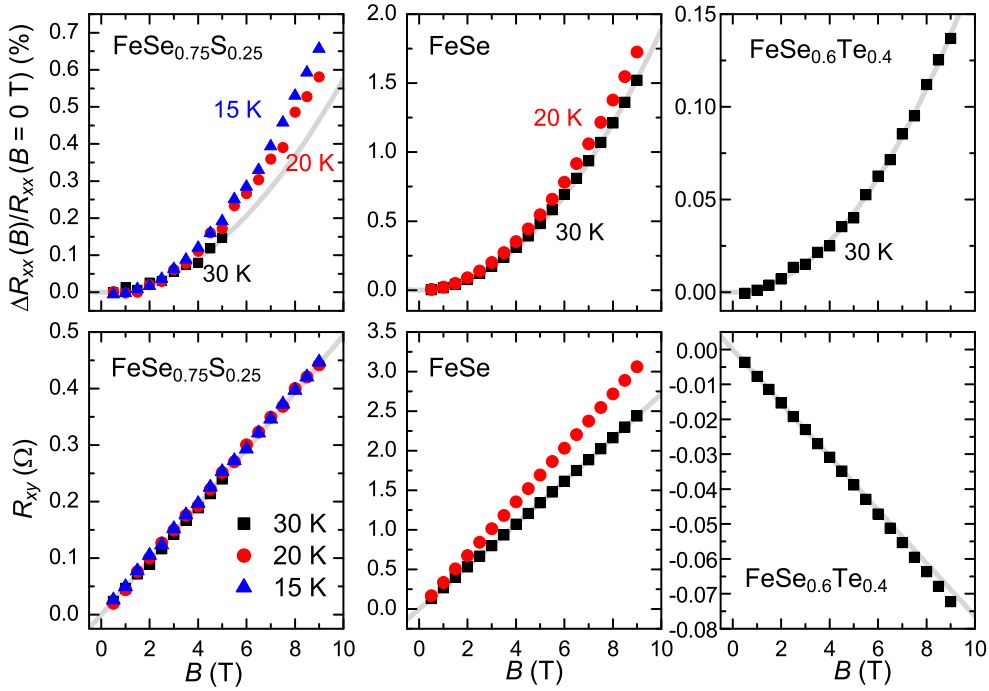

FIG. 3. Magnetoresistance, $[\rho(B) - \rho(0\ \mathrm{T})]/\rho(0\ \mathrm{T})$ (upper panels), and Hall resistance, $R_{xy}(B)$ (lower panels), as a function of the magnetic field of FeSe (center), $x = 0.25$ (left) and $y = 0.4$ (right) films at 15 K (blue triangle), 20 K (red circle), and 30 K (black square). The gray lines are the fitted curves for these data by the general two-carrier model.

substitution. R_{H} at low temperatures was large even after the structural transition disappeared for S substitution. The R_{H}-vs-T behaviors of the S-substituted films are similar to those of bulk samples [23,24], while that of the FeSe film is different from that of bulk FeSe [25,26]. No clear signature of the possible antiferromagnetic transition was observed in R_{H}.

We should note that the R_{H} behavior at low temperatures of the FeSe film is different from that of bulk single crystals; R_{H} becomes negative at low temperatures for the bulk sample, while that of our FeSe film remains positive. We would like to point out, however, that the difference in R_{H} at low temperatures is an irrelevant factor to discuss the superconductivity of this material. In fact, an FeSe film on CaF_2 shows a positive R_{H} value in the low-temperature limit, but its T_{c} is higher than that of bulk samples. This result indicates that the sign of R_{H} in the low-temperature limit hardly affects the T_{c} values. Furthermore, we previously observed a systematic strain dependence of the carrier density in both our films and our bulk samples by the same analysis as in the present paper [20]. This indicates that the sign of R_{H} in the low-temperature limit hardly affects our conclusion. The negative R_{H} in the low-temperature limit in bulk crystals is attributed to the high mobility of an electron-type carrier [26]. The origin of high mobility is believed to be an electron-type carrier in a Dirac-cone-like band near the M point of the Brillouin zone, which appears below $T_{\mathrm{s}} = 90$ K. When the lattice parameters change even slightly by the introduction of the strain, the contribution of the high-mobility carrier originating from the Dirac cone changes. This strongly affects the low-temperature R_{H} values. Even when the mobility of electrons changes, carrier density does not change considerably, which is probed by the Hall effect study in both in bulk and films [20], indicating that the difference in the R_{H} behavior at low temperature does not affect our conclusion in the present case.

In order to investigate the nature of charge carriers in the films we also performed magnetoresistance measurements. Figure 3 shows the magnetoresistance, $[\rho(B) - \rho(0\ \mathrm{T})]/\rho(0\ \mathrm{T})$, and the Hall resistance, $R_{xy}(B)$, as a function of the magnetic field of FeSe, $x = 0.25$ and $y = 0.4$ films. The magnetoresistance and Hall resistance shows B^2 and B-linear behaviors, respectively, for all samples. Negative magnetoresistance due to weak localization was not observed even for $T = 15$ K data of the $x = 0.25$ sample, which may support the supposition that the upturn behavior in the R-vs-T curve observed for the $x = 0.25$ film below 20 K is caused by the magnetic transition.

In a multiband system like iron chalcogenides both electron- and hole-type carriers contribute to the electric conduction. We considered one electron band and one hole band representing the multiple bands and applied the textbook approach for multiband materials. In a classical two-carrier model, the conductivity tensor is expressed as $\sigma_{xx} = \frac{en_{\mathrm{e}}\mu_{\mathrm{e}}}{1+(\mu_{\mathrm{e}}B)^2} + \frac{en_{\mathrm{h}}\mu_{\mathrm{h}}}{1+(\mu_{\mathrm{h}}B)^2}$ and $\sigma_{yx} = -\frac{en_{\mathrm{e}}\mu_{\mathrm{e}}^2 B}{1+(\mu_{\mathrm{e}}B)^2} + \frac{en_{\mathrm{h}}\mu_{\mathrm{h}}^2 B}{1+(\mu_{\mathrm{h}}B)^2}$, where n_{h}, n_{e}, μ_{h}, and μ_{e} are the hole density, the electron density, the hole mobility, and the electron mobility, respectively. The validity of application of the two-carrier model to iron chalcogenides has been confirmed by a recent terahertz Faraday rotation measurement, where the two-carrier model perfectly reproduced the measured $\sigma_{xx}(\omega)$ and $\sigma_{yx}(\omega)$ [27]. The observed B^2 and B-linear behaviors of the magnetoresistance and Hall resistance can be reproduced by the low-field limit

expression of the two-carrier model, where the resistivity tensor is written as

$$\rho_{xx}(0) = \frac{1}{e(n_h\mu_h + n_e\mu_e)}, \quad (1)$$

$$\frac{\rho_{xx}(B) - \rho_{xx}(0)}{\rho_{xx}(0)} = \frac{n_h n_e \mu_h \mu_e (\mu_h + \mu_e)^2}{(n_h\mu_h + n_e\mu_e)^2} B^2, \quad (2)$$

$$\rho_{yx}(B) = \frac{n_h\mu_h^2 - n_e\mu_e^2}{e(n_h\mu_h + n_e\mu_e)^2} B. \quad (3)$$

In order to determine the carrier densities and mobilities by these equations, we used the reported values of the ratio of electron density, $n_e/(n_e + n_h)$. The terahertz measurement revealed that $n_e/(n_e + n_h) \sim 0.25$ for an FeSe film on LAO [27]. $n_e/(n_e + n_h) = 0.5$ was suggested for 50%–60% Te-substituted samples by an angle-resolved photoemisson spectroscopy (ARPES) measurement with bulk crystals and Hall effect study with thin films [28,29]. In addition, S substitution does not significantly change this ratio, which was revealed by a magnetotransport measurement with bulk samples [30]. Although there is no report on the ratio of the carrier densities for Fe(Se,S) films, an ARPES study revealed that the ratio of the carrier densities is almost the same among bulk and films under compressive and tensile strain [31], and it is reasonable to assume that this is also the case with S-substituted samples. Therefore, we took $n_e/(n_e + n_h) = 0.25$ for the FeSe film and S-substituted samples, and also assumed $n_e/(n_e + n_h) = 0.5$ for a Te-60% sample and took the linear-interpolated values for other Te-substituted samples.

Figure 4 shows the results of the analysis with the two-carrier model as a function of the composition of the films. We confirmed the validity of the low-field-limit expression of the model for the obtained parameters in the measured range by putting them into the general expression of the model, as shown in Fig. 3, where gray curves represent those for the general expression. For S substitution, the carrier densities were almost constant, independent of the S content, while the hole and electron mobilities decreased with increasing the substituting amount. An ARPES measurement for bulk $FeSe_{1-x}S_x$ revealed that the Fermi surface becomes large for samples in the tetragonal phase [11]. Such an increase in carrier densities was not observed in the present study, which might be due to the difference between energy regions probed by ARPES and transport measurements. For Te substitution, on the other hand, the carrier densities largely increased with increasing Te content; the $y = 0.4$ film have n_h more than 1.5-2 times larger than that of the FeSe film. Even though there is ambiguity in the result for the Te-substituted samples depending on what kind of interpolation is adopted, we can safely conclude that carrier densities for the Fe(Se,Te) samples in the tetragonal phase are larger than those for samples in the orthorhombic phase. The mobilities decreased with increasing Te content, the same as S substitution. Thus, we observed a contrasting behavior of the carrier densities between S and Te substitution; the carrier densities increased with increasing Te content, while no significant change was observed for S substitution. This composition dependence of the carrier densities well corresponds to the change of the T_c values. Therefore, this result indicates

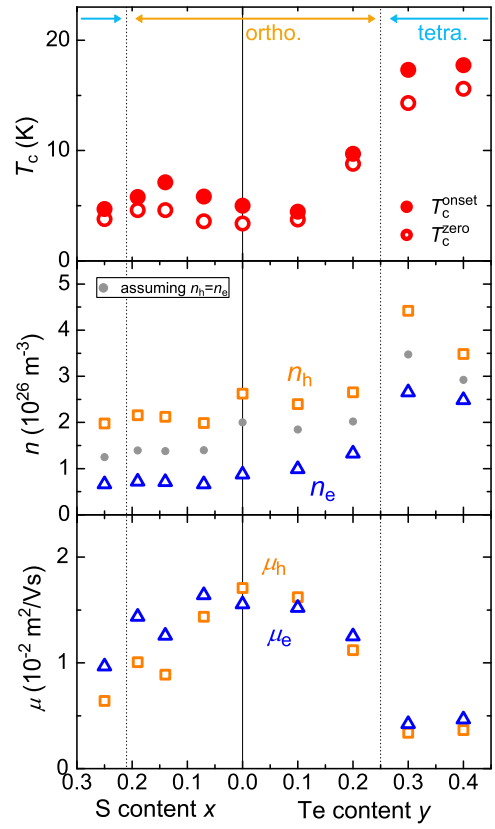

FIG. 4. Results of the analysis with the two-carrier model. The composition dependence of the superconducting transition temperature, T_c (top), the carrier densities, n_h and n_e, at 30 K (middle), and the mobilities, μ_h and μ_e at 30 K (bottom). The dotted lines show the ortho-tetra boundaries.

a correlation between the carrier densities and T_c in our films.

A similar correlation between T_c and carrier density was observed in FeSe films under various degrees of lattice strain, from tensile to compressive strain [20,31,32]. As the in-plane strain became more compressed, we observed the decrease of the structural transition temperature (and also the decrease of the band splitting energy due to nematicity), the increase of T_c, and the increase of both electron and hole densities. The change of the carrier densities depending on the strain is the so-called self-doping induced by the strain [33]. Similar to the results for the samples with different compositions, higher T_c is observed for samples with larger carrier densities in the case of FeSe films under various degrees of strain; an FeSe film with T_c of 12 K shows approximately two times larger carrier densities than FeSe films with $T_c < 2$ K. These results suggest the relation between T_c and the carrier densities in iron chalcogenides.

We already mentioned, based on our results, that the electronic nematicity does not have universal significance in superconductivity in iron chalcogenides [17]. The difference of the behavior of the carrier densities between Te and S substitution suggests that the structural transition affects the electronic structure in a different manner between $FeSe_{1-y}Te_y$ and $FeSe_{1-x}S_x$. This would be the direct origin of the difference of T_c behavior at the end point of the orthorhombic

phase, manifested in the correlation between T_c and the carrier densities.

It is very interesting that our results that the increase of carrier density is important for high T_c is similar to the results of a field-effect-transistor experiment with FeSe, where T_c increased with increasing electron density [34]. Electron-doped FeSe which shows $T_c = 40$ K is likely to have only electron Fermi surfaces, as was observed in an intercalated FeSe [35]. Naively thinking, the mechanism of the superconductivity in the heavily-electron-doped FeSe will be different from that of nondoped FeSe. Further research will be needed to compare the superconductivities in these two material systems.

IV. CONCLUSIONS

In conclusion, we comparatively investigated the transport properties of $FeSe_{1-x}S_x$ and $FeSe_{1-y}Te_y$ thin films under magnetic fields. Enhancement of the Hall coefficient, R_H, of FeSe films at low temperatures was reduced by both S and Te substitution. Fe(Se,Te) showed small R_H values near zero at low temperatures in the tetragonal phase, while R_H values remained rather large for Fe(Se,S). The analysis of the magnetoresistance and the Hall resistance using a classical two-carrier model revealed that the carrier densities of the films increased with increasing Te content, while no significant change was observed for the S substitution. This suggests that the structural transition affects the electronic structure differently between Fe(Se,S) and Fe(Se,Te). The correlation between T_c and the carrier densities indicates this fact is the direct cause of the difference in the T_c behaviors at the end point of the structural transition.

ACKNOWLEDGMENTS

We would like to thank K. Ueno for the x-ray diffraction measurements of the films. We also thank M. Hanawa for the thickness measurements of the films. This research was supported by the Murata Science Foundation and JSPS KAKENHI Grants No. 18H04212 and No. 19K14651.

[1] Y. Kamihara, T. Watanabe, M. Hirano, and H. Hosono, J. Am. Chem. Soc. **130**, 3296 (2008).
[2] F. C. Hsu, J. Y. Luo, K. W. Yeh, T. K. Chen, T. W. Huang, P. M. Wu, Y. C. Lee, Y. L. Huang, Y. Y. Chu, D. C. Yan, and M. K. Wu, Proc. Natl. Acad. Sci. USA **105**, 14262 (2008).
[3] T. M. McQueen, A. J. Williams, P. W. Stephens, J. Tao, Y. Zhu, V. Ksenofontov, F. Casper, C. Felser, and R. J. Cava, Phys. Rev. Lett. **103**, 057002 (2009).
[4] T. Shimojima, Y. Suzuki, T. Sonobe, A. Nakamura, M. Sakano, J. Omachi, K. Yoshioka, M. Kuwata-Gonokami, K. Ono, H. Kumigashira, A. E. Böhmer, F. Hardy, T. Wolf, C. Meingast, H. v. Löhneysen, H. Ikeda, and K. Ishizaka, Phys. Rev. B **90**, 121111(R) (2014).
[5] K. Nakayama, Y. Miyata, G. N. Phan, T. Sato, Y. Tanabe, T. Urata, K. Tanigaki, and T. Takahashi, Phys. Rev. Lett. **113**, 237001 (2014).
[6] R. M. Fernandes, A. V. Chubukov, and J. Schmalian, Nat. Phys. **10**, 97 (2014).
[7] A. E. Böhmer and A. Kreisel, J. Phys.: Condens. Matter **30**, 023001 (2018).
[8] M. D. Watson, T. K. Kim, A. A. Haghighirad, S. F. Blake, N. R. Davies, M. Hoesch, T. Wolf, and A. I. Coldea, Phys. Rev. B **92**, 121108(R) (2015).
[9] M. Abdel-Hafiez, Y. J. Pu, J. Brisbois, R. Peng, D. L. Feng, D. A. Chareev, A. V. Silhanek, C. Krellner, A. N. Vasiliev, and X.-J. Chen, Phys. Rev. B **93**, 224508 (2016).
[10] S. Hosoi, K. Matsuura, K. Ishida, H. Wang, Y. Mizukami, T. Watashige, S. Kasahara, Y. Matsuda, and T. Shibauchi, Proc. Natl. Acad. Sci. USA **113**, 8139 (2016).
[11] P. Reiss, M. D. Watson, T. K. Kim, A. A. Haghighirad, D. N. Woodruff, M. Bruma, S. J. Clarke, and A. I. Coldea, Phys. Rev. B **96**, 121103(R) (2017).
[12] Y. Sato, S. Kasahara, T. Taniguchi, X. Xing, Y. Kasahara, Y. Tokiwa, Y. Yamakawa, H. Kontani, T. Shibauchi, and Y. Matsuda, Proc. Natl. Acad. Sci. USA **115**, 1227 (2018).
[13] T. Hanaguri, K. Iwaya, Y. Kohsaka, T. Machida, T. Watashige, S. Kasahara, T. Shibauchi, and Y. Matsuda, Sci. Adv. **4**, eaar6419 (2018).
[14] M. H. Fang, H. M. Pham, B. Qian, T. J. Liu, E. K. Vehstedt, Y. Liu, L. Spinu, and Z. Q. Mao, Phys. Rev. B **78**, 224503 (2008).
[15] Y. Imai, Y. Sawada, F. Nabeshima, and A. Maeda, Proc. Natl. Acad. Sci. USA **112**, 1937 (2015).
[16] Y. Imai, Y. Sawada, F. Nabeshima, D. Asami, M. Kawai, and A. Maeda, Sci. Rep. **7**, 46653 (2017).
[17] F. Nabeshima, T. Ishikawa, O. Ken-ichi, M. Kawai, and A. Maeda, J. Phys. Soc. Jpn. **87**, 073704 (2018).
[18] Y. Imai, R. Tanaka, T. Akiike, M. Hanawa, I. Tsukada, and A. Maeda, Jpn. J. Appl. Phys. **49**, 023101 (2010).
[19] Y. Imai, T. Akiike, M. Hanawa, I. Tsukada, A. Ichinose, A. Maeda, T. Hikage, T. Kawaguchi, and H. Ikuta, Appl. Phys. Express **3**, 043102 (2010).
[20] F. Nabeshima, M. Kawai, T. Ishikawa, N. Shikama, and A. Maeda, Jpn. J. Appl. Phys. **57**, 120314 (2018).
[21] J. P. Sun, K. Matsuura, G. Z. Ye, Y. Mizukami, M. Shimozawa, K. Matsubayashi, M. Yamashita, T. Watashige, S. Kasahara, Y. Matsuda, J. Q. Yan, B. C. Sales, Y. Uwatoko, J. G. Cheng, and T. Shibauchi, Nat. Commun. **7**, 12146 (2016).
[22] Y. Sawada, F. Nabeshima, Y. Imai, and A. Maeda, J. Phys. Soc. Jpn. **85**, 073703 (2016).
[23] Y. Sun, S. Pyon, and T. Tamegai, Phys. Rev. B **93**, 104502 (2016).
[24] Y. A. Ovchenkov, D. A. Chareev, D. E. Presnov, O. S. Volkova, and A. N. Vasiliev, J. Low Temp. Phys. **185**, 467 (2016).
[25] S. Kasahara, T. Watashige, T. Hanaguri, Y. Kohsaka, T. Yamashita, Y. Shimoyama, Y. Mizukami, R. Endo, H. Ikeda, K. Aoyama, T. Terashima, S. Uji, T. Wolf, H. von Löhneysen, T. Shibauchi, and Y. Matsuda, Proc. Natl. Acad. Sci. USA **111**, 16309 (2014).

[26] K. K. Huynh, Y. Tanabe, T. Urata, H. Oguro, S. Heguri, K. Watanabe, and K. Tanigaki, Phys. Rev. B **90**, 144516 (2014).

[27] N. Yoshikawa, M. Takayama, N. Shikama, T. Ishikawa, F. Nabeshima, A. Maeda, and R. Shimano, Phys. Rev. B **100**, 035110 (2019).

[28] I. Tsukada, F. Nabeshima, A. Ichinose, S. Komiya, M. Hanawa, Y. Imai, and A. Maeda, Jpn. J. Appl. Phys. **54**, 043102 (2015).

[29] A. Tamai, A. Y. Ganin, E. Rozbicki, J. Bacsa, W. Meevasana, P. D. C. King, M. Caffio, R. Schaub, S. Margadonna, K. Prassides, M. J. Rosseinsky, and F. Baumberger, Phys. Rev. Lett. **104**, 097002 (2010).

[30] Y. A. Ovchenkov, D. A. Chareev, V. A. Kulbachinskii, V. G. Kytin, D. E. Presnov, O. S. Volkova, and A. N. Vasiliev, Supercond. Sci. Technol. **30**, 035017 (2017).

[31] G. N. Phan, K. Nakayama, K. Sugawara, T. Sato, T. Urata, Y. Tanabe, K. Tanigaki, F. Nabeshima, Y. Imai, A. Maeda, and T. Takahashi, Phys. Rev. B **95**, 224507 (2017).

[32] Z. Feng, J. Yuan, J. Li, X. Wu, W. Hu, B. Shen, M. Qin, L. Zhao, B. Zhu, V. Stanev, M. Liu, G. Zhang, X. Dong, F. Zhou, X. Zhou, I. Takeuchi, Z. Zhao, and K. Jin, arXiv:1807.01273.

[33] E. J. Moon, J. M. Rondinelli, N. Prasai, B. A. Gray, M. Kareev, J. Chakhalian, and J. L. Cohn, Phys. Rev. B **85**, 121106(R) (2012).

[34] B. Lei, J. H. Cui, Z. J. Xiang, C. Shang, N. Z. Wang, G. J. Ye, X. G. Luo, T. Wu, Z. Sun, and X. H. Chen, Phys. Rev. Lett. **116**, 077002 (2016).

[35] X. H. Niu, R. Peng, H. C. Xu, Y. J. Yan, J. Jiang, D. F. Xu, T. L. Yu, Q. Song, Z. C. Huang, Y. X. Wang, B. P. Xie, X. F. Lu, N. Z. Wang, X. H. Chen, Z. Sun, and D. L. Feng, Phys. Rev. B **92**, 060504(R) (2015).